18th Brazilian Congress of Thermal Sciences and Engineering
November 16-20, 2020 (Online)

ENC-2020-0541
BIOGAS-FUELED MICRO GAS TURBINE THERMODYNAMIC ANALYSIS

Gustavo Sana Trindade
Luís Antônio Bortolaia
Federal University of Ouro Preto - University Campus, Morro do Cruzeiro. CEP: 35400-000, Ouro Preto, Minas Gerais, Brazil.
gustavo.trindade@aluno.ufop.edu.br, luis.bortolaia@ufop.edu.br
Elisângela Martins Leal
Federal University of Ouro Preto - University Campus, Morro do Cruzeiro. CEP: 35400-000, Ouro Preto, Minas Gerais, Brazil.
elisangelamleal@ufop.edu.br

Abstract. *The generation of electricity through biogas produced from municipal solid waste has become an effective option for diversification Brazilian electricity sector. Therefore, in order to ratify this trend, a thermodynamic analysis of a 100 kWe micro gas turbine using biogas as fuel are presented in this paper. In terms of methodology, a classic steady state thermodynamic model and parametric analysis were used to evaluate the equipment performance. Engineering Equation Solver Demo (EES) was the software used to run compressor, combustor, turbine and recuperator models. Besides the iterative calculation and the parametric graphic construction, it has the advantage of containing thermodynamic relationships for many fluids in its internal routines. A sensitivity analysis was performed by varying pressure ratio, turbine inlet temperature and compressor, turbine and recuperator efficiencies to quantify and compare important parameters such as thermal efficiency and specific fuel consumption and, thus, determine the best operation point. The results showed that the regenerative cycle has the highest efficiency at a turbine inlet temperature of 1200 K at a pressure ratio equal to 4 and compressor efficiency of 0.81, turbine efficiency of 0.84, and a 0.85 regenerator efficiency. The electrical efficiency obtained were on the range of 25% to 32%.*

Keywords: *micro gas turbine, biogas, thermodynamic modeling, electrical efficiency, specific fuel consumption.*

1. INTRODUCTION

Recent work (MosayebNezhad et al., 2019) states that the world demand of energy will undoubtedly increase due to population growth, especially in large urban centers. Moreover, the use of fossil fuels as a primary source for power generation over many years has led to a series of very worrisome environmental degradations such as ozone layer depletion (Adefarati and Bansal, 2016). Thus, several regulations have recently been created and the development of technologies associated with sources of renewable, clean, non-depleting and sustainable energy economically viable has become essential (Adefarati and Bansal, 2017), as has been ratified in 2015 Paris agreement.

In this context, according to Somehsaraei et al. (2014) micro gas turbines (MGTs), which are usually defined as small gas turbines up to a few hundred kilowatts, are considered as promising power generators since provide high fuel flexibility, low emissions, small footprint, and low maintenance costs what makes it commercially interesting. And according to Gupta et al. (2010) the MGT system might be especially interesting when fueled by green biogas. Despite the lower heating value of the biogas, which impacts the performance and the operating conditions of the MGT, the current technology, more mature, allows modifications so that the equipment works as well as fed with various fuels. As said MosayebNezhad et al. (2019), one method to compensate the low energy content of biogas is increase mass flow rate through the MGT to achieve the same thermal loads that could be otherwise attained using gaseous fossil fuels. Another concern about fuel changes is the performance impact of other machine components, such as compressor, which need to operate at conditions that deviate from the original design. Compressor surge is a particular concern when firing low heating value fuels such as biogas. However, according to Somehsaraei et al. (2014), in contrast to large-scale gas turbines, the surge problem in MGT systems does not seem to be very critical when fed by biogas and a lot of current lines of research, referenced in this authors paper, investigate and corroborate that.

All living matter is decomposed by bacteria after death, which takes the energy necessary to survive from biomass and release gases and heat into the atmosphere. This gas is the biogas, basically composed of methane (CH_4) and carbon dioxide (CO_2), an abundant, non-polluting and cheap source. Biogas can be obtained from solid urban waste, as well as agriculture waste or even animal excrement. The energetic potential of biogas depends on methane concentration contained in the gas, which determines its calorific value. The methane content varies from 40 to 75% depending on the generating source. The generation of biogas (and subsequently electricity by the microturbine) from solid urban waste can occur through various processes, such as burning biogas recovered from garbage dumps, incineration or gasification. As the combination of biogas-MGT has emerged as a profitable match, especially for distributed power generation, a growing interest in the utilization of biogas in the MGT system is noticeable in scientific literature (Somehsaraei et al., 2014).

Despite many researches related to the use of biogas as fuel are happening in last decade, few studies deal in detail, step by step, the thermodynamic modeling of a micro gas turbine fueled with it. Thus, a scientific novelty is presented in this work in order to expand research and knowledge in this engineering area so important around the world and in Brazilian scenario too.

2. MICRO GAS TURBINE: THERMODYNAMIC MODELING

A microturbine is a smaller scale gas turbine (output less than 500 kWe), that is, a turbomachine based on a Brayton cycle that transfers energy from fluid to the rotor and converts it into kinetic energy and the work output as shaft was used for different purposes. The process of scaling down a gas turbine is not as easy as it looks like, it possess great difficulties. These gas turbines are used for power generation; also they can be used for distributed power supply system. These micro gas turbines have also found its application in cogeneration systems, which supply steam and power at the same time (Shukla, 2013). The sketch of a regerenative microturbine is represented in Fig. 1.

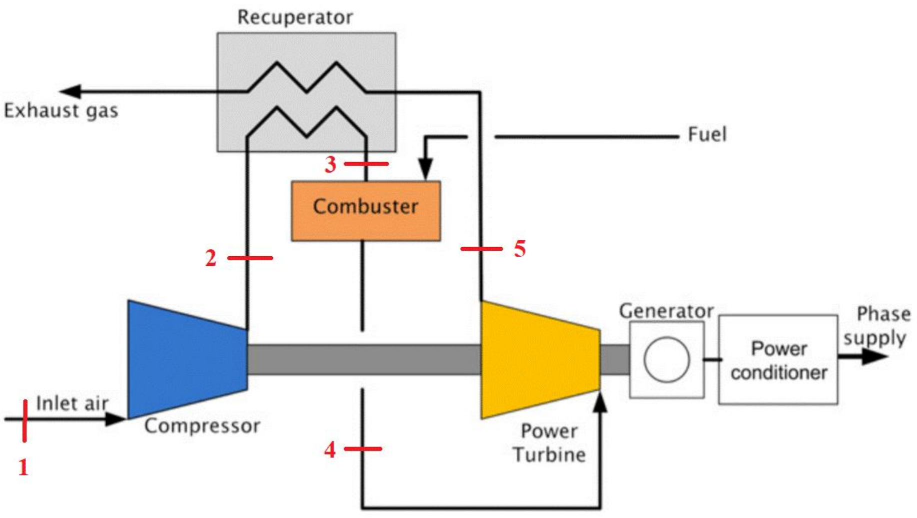

Figure 1. Block diagram of a gas microturbine.
Adapted from: Ismail et al. (2013)

Next, the function and the thermodynamic math models of each component will be presented.

2.1 Compressor

At cycle beginning, air under ambient conditions is admitted in a compressor where its pressure is increased along with temperature. The pressure ratio is defined as the ratio between the outlet (P_2) and inlet pressure (P_1). The inlet pressure is equal to the ambient pressure minus a pressure drop due to an air filter always installed in intake duct. The ideal compression/expansion process is adiabatic and irreversible, therefore isentropic. However, there is always a degree of irreversibility and in a compressor case it's measured with a parameter called compressor isentropic efficiency (η_c), defined by Eq. (1):

$$\eta_c = \frac{h_{2s}-h_1}{h_2-h_1} \tag{1}$$

h_1, h_2 and h_{2s} are the compressor inlet, outlet and outlet isentropic process enthalpies, respectively, given in kJ/kg and always functions of temperature.

The compression power ($\dot{W}_c$) is given in kW by Eq. (2):

$$\dot{W}_c = \dot{m}_a \frac{h_2-h_1}{\eta_m} \tag{2}$$

η_m is the mechanical efficiency and $\dot{m}_a$ the flow mass rate in kg/s that will be more detailed in combustor analysis.

2.2 Recuperator

Recuperators are heat exchangers that preheat compressed air by recovering heat from exhaust gas of turbines, thus reducing fuel consumption and improving the system efficiency, typically from 16–20% to 30% . A recuperator with high effectiveness and low pressure loss is mandatory for a good performance (Xiao et. al, 2017). The recuperator efficiency (η_{rec}) is defined by Eq. (3):

$$\eta_{rec} = \frac{T_3 - T_2}{T_5 - T_2} \tag{3}$$

T represents temperatures, in K. The subscripts *3* and *5* indicate recuperator and turbine outlet states, respectively.

2.3 Combustor

The compressed air is then mixed with fuel and the mixture is burnt in a combustion chamber, where its energy gets increased. The combustor treatment is perfomed as suggested by Borglin (1991), which combustor outlet air is divided into two parts: stoichiometric combustion air and excess air. The air stoichiometric combustion process with fuel produces stoichiometric gas. Thereby, instead combustion gas leaving combustor, it is treated as a mixture of stoichiometric gas and excess air.

As biogas is mainly composed by methane (CH_4) and carbon dioxide (CO_2), the chemical stoichiometric combustion reaction is represented by Eq. (4):

$$\mathrm{aCH4} + \mathrm{bCO2} + Q_{est}(\mathrm{O2} + 3{,}76\mathrm{N2}) \rightarrow \mathrm{xCO2} + \mathrm{yH2O} + \mathrm{zN2} \tag{4}$$

a, *b*, *x*, *y*, *z* and Q_{est} are the number of moles of each substance. From balancing, Eq. (5), Eq. (6), Eq. (7) and Eq. (8) are obtained:

$$\mathrm{x} = \mathrm{a} + \mathrm{b} = 1 \tag{5}$$

$$\mathrm{y} = 2\mathrm{a} \tag{6}$$

$$Q_{est} = 2\mathrm{a} \tag{7}$$

$$\mathrm{z} = 7{,}52\mathrm{a} \tag{8}$$

For stoichiometric reaction the air fuel ratio (AFR_{est}) is defined by Eq. (8):

$$AFR_{est} = \frac{m_a}{m_f} = GFR_{est} - 1 \tag{9}$$

GFR_{est} is the gas fuel ratio and air mass (m_a) and fuel mass (m_f) in kg are given by Eq. (10) and Eq. (11), respectively:

$$m_a = (1 + 3{,}76)\mathrm{Q}_{est} M_a \tag{10}$$

$$m_f = \mathrm{aM}_{CH4} + \mathrm{bM}_{CO2} \tag{11}$$

M is the molecular mass of each substance in kg/kmol.

Other important parameters are the fuel air ratio (Fa) given by the Eq. (12)

$$Fa = \frac{h_{4a} - h_3}{LHV_f - (GFR_{est} h_{4g} - AFR_{est} h_{4a})} \tag{12}$$

Fa is obtained from energy balance in combustor. *LHV* is the lower heat value in kJ/kg and the subscripts *4*, *a*, *g* indicate outlet combustor state, air and combustion gas, respectively. h_{4g} is calculated by Eq. (13):

$$h_{4g} = f(T_4, P_4, a) = Y_{CO2} h_{CO2} + Y_{H20} h_{H20} + Y_{N2} h_{N2} \tag{13}$$

Y is the molar fraction of each substance.

The composition characterization of combustion gas is realized by the stoichiometric gas ratio (SGR) definition given by Eq. (14):

$$SGR = \frac{\dot{m}_{sg}}{\dot{m}_{cg}} = \frac{GFR_{est}Fa}{1+Fa} \tag{14}$$

$\dot{m}_{sg}$ and $\dot{m}_{cg}$ are stoichiometric gas mass flow and combustion gas mass flow, respectively, in kg/s. *SGR* equals one means stoichiometric gass and equals zero pure air.

Finally, the combustor outlet enthalpy (h_4), an essential design variable, can be calculated as shown in Eq. (15):

$$h_4 = SGRh_{4g} + (1 - SGR)h_a \tag{15}$$

Ultimately, the combustion heat ($\dot{Q}$), in kW, is calculated by Eq. (16):

$$\dot{Q} = \dot{m}_f LHV_f = a\,\dot{m}_a\,Fa\,LHV_{CH4} \tag{16}$$

The air flow mass rate is a function of the required electrical power ($\dot{W}_{el}$) in kW, the specific turbine/compressor work (w_t and w_c) in kJ/kg, the electrical efficiency (η_{el}) and the fuel air ratio as shown in Eq. (17):

$$\dot{m}_a = \frac{\dot{W}_{el}}{(1+\mathrm{Fa})(w_t - w_c)\eta_{el}} \tag{17}$$

The difference between w_t and w_c is the cycle liquid specific work, w_l, since compressor and turbine are both mounted on the same shaft.

2.4 Turbine

In turbine the gas is allowed to work and the transformation energy takes place. As well as compression process, there are irreversibilities in expansion processes and in a turbine case it's measured with a parameter called turbine isentropic efficiency (η_t), defined by Eq. (18):

$$\eta_t = \frac{h_4 - h_5}{h_4 - h_{5s}} \tag{18}$$

The subscript 5 indicates turbine outlet state. As in turbine the working fluid is a mixture and EES library functions are just for single substance fluids, the calculation of T_{5s} and T_5, which depend on s_{5s} (specific entropy on state *5s*, in kJ/kgK) and h_5, respectively, must be done with the definition of each property. According to Malinowski et al. (2013), increase in specific entropy and enthalpy of the working gas between states *i* and *j* are calculated from Eq. (19) and (20), respectively:

$$\Delta s = \int_{T_i}^{T_j} \frac{C_p(T)}{T} dT - Rln(\frac{P_j}{P_i}) \tag{19}$$

$$\Delta h = \int_{T_i}^{T_j} C_p(T)\, dT \tag{20}$$

The constant-pressure specific heat, C_p, in kJ/kgK, according to Çengel and Boles (2006), can be calculated by Eq. (21):

$$C_p(T) = \alpha + \beta T + \gamma T^2 + \delta T^3 \tag{21}$$

The necessary coefficients α, β, γ, δ are also presented in Çengel and Boles (2006).

Is important to note that the integration must be done for each substance. Thereby, the analogous weighting shown in Eq. (14) and Eq. (15) must be done for specific entropy and enthalpy calculation. The same must be done to determine gas constant, *R*, in J/kgK.

Thus, under known enthalpies, the turbine power ($\dot{W}_t$) is given in kW by Eq. (22):

$$\dot{W}_t = (\dot{m}_a + \dot{m}_f)(h_4 - h_5) \tag{22}$$

Lastly, other important parameter is the specific fuel consumption (*SFC*), measured in kg/kW.h, calculated by Eq. (23):

$$\mathrm{SFC} = \frac{3600\,Fa}{w_l} \tag{23}$$

3. METHODOLOGY

From presented equation and internal computational thermodynamic tables, a program was elaborated in Solver EES to calculate the desired parameters and then analyze the influence between them through parametric tables and graphics. The values of input parameters are shown in the Tab. 1. The desired output parameters are: outlet turbine temperature, specific fuel consumption, air flow mass rate, compressor work, combustion heat, electrical efficiency (η_e) given by Eq. (20) and thermal efficiency (η_{th}), latter given by Eq. (21):

$$\eta_e = \frac{\dot{W}_e}{\dot{Q}} \tag{20}$$

$\dot{W}_e$ represents the electrical power in kW.

$$\eta_{th} = \frac{\dot{W}_t - \dot{W}_c}{\dot{Q}} \tag{21}$$

Table 1. Values of input parameters

Parameters	Value, range considered or consideration
Ambient Temperature (K)	288
Atmospheric Pressure (kPa)	101.3
Combustion efficiency	0.98
Compressor isentropic efficiency	0.79;0.80;0,81[(2)]
Electrical efficiency	0.96
Electrical power (kW)	100
Lower Heat Value of CH_4 (kJ/kg)	50050[(1)]
Mechanical efficiency of compressor and turbine	0.98
Pressure air drop at combustor (% of recuperator outlet pressure)	2
Pressure air drop at recuperator (% of compressor outlet pressure)	3
Pressure drop at compressor inlet (% of atmospheric pressure)	1
Pressure combustion gas drop recuperator (% of turbine outlet pressure)	2
Pressure combustion gas drop at pipe after recuperator (% of turbine outlet pressure)	1
Compressor pressure ratio	3.5;4.0;4.5;5.0
Recuperator efficiency	0.75;0.80;0.85
Turbine Inlet Temperature (K)	1000;1100;1200
Turbine isentropic efficiency	0.82;0.83;0,84[(2)]
Volume composition of biogas (% CH_4)	60

[(1)] Çengel and Boles, 2006
[(2)] Malinowsky et al., 2013

4. RESULTS AND DISCUSSION

Always some parameters were fixed to evaluate the influence between others, as described in methodology section. Initially, the research done was to evaluate turbine outlet temperature according to compressor pressure ratio variation. The result is shown in Fig. 2:

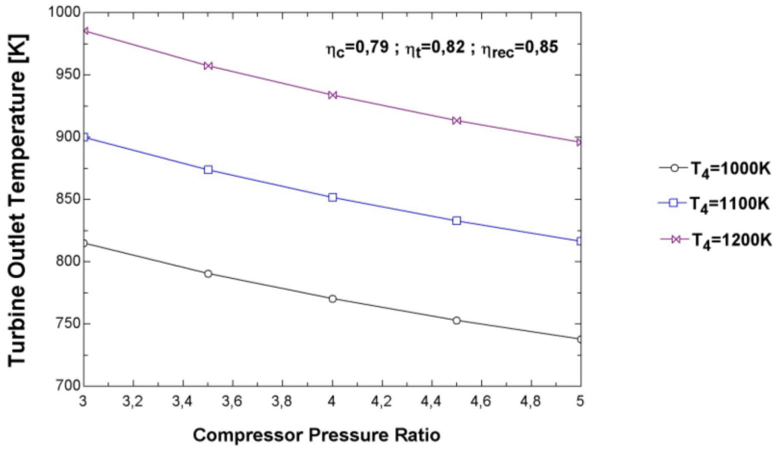

Figure 2. Turbine outlet temperature versus compressor pressure ratio.

From the figure, it can be seen a decrease in turbine outlet temperatures as compressor pressure ratio increases, as expected. This occurs because an increase in pressure ratio causes an increase in turbine expansion ratio.

Recuperator outlet air temperature increases as turbine inlet temperature increases since T_5 increases too and a higher heat transfer occurs in recuperator and it decreases as increase compressor pressure ratio, since outlet compressor temperature increases and the heat exchange with combustion gases decreases as noted in Fig. 3. Therefore, it is also expected that specific fuel consumption increases too as shown in Fig. 4.

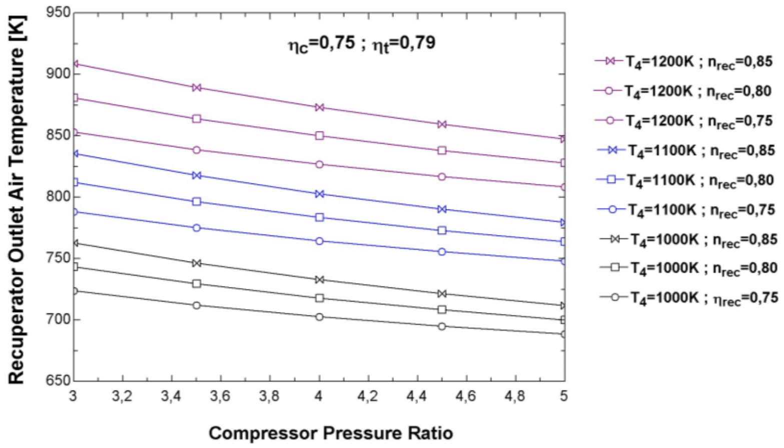

Figure 3. Recuperator outlet air temperature versus compressor pressure ratio.

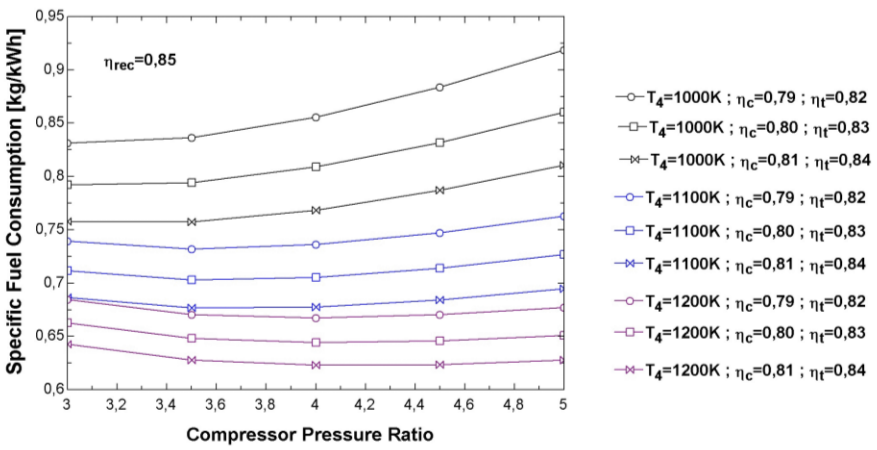

Figure 4. Specific fuel consumption versus compressor pressure ratio.

Thus, to reduce specific fuel consumption, engineers are always looking to increase components efficiencies and turbine inlet temperature.

For further liquid power, combustion heat and consequent cycle efficiencies analysis air mass flow needs to be investigated. The results is shown in Fig. 5:

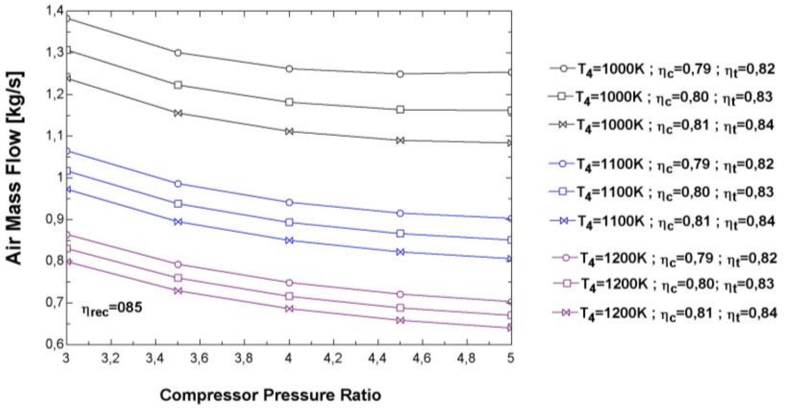

Figure 5. Air mass flow versus compressor pressure ratio.

As specific fuel consumption, air mass flow is lower for higher temperatures and efficiencies and presents inverse behavior with compressor pressure ratio, because for higher compressor pressure ratio, recuperator outlet temperature decreases and less air excess is required to achieve the same combustion temperature. In sequence, Fig. 6 and Fig. 7 shows results for liquid power and combustion heat, respectively.

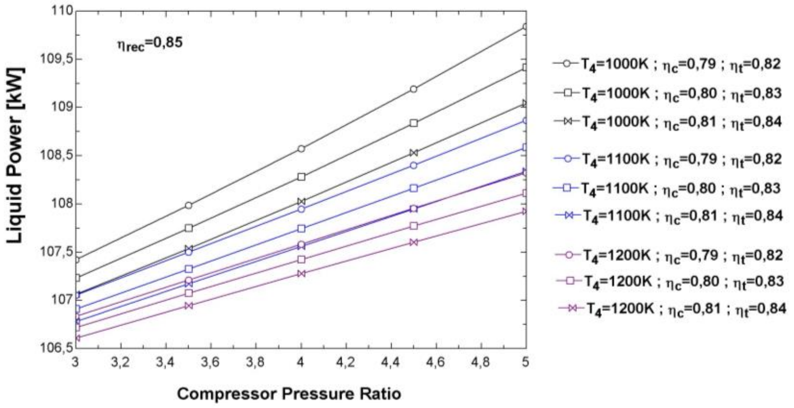

Figure 6. Liquid power versus compressor pressure ratio.

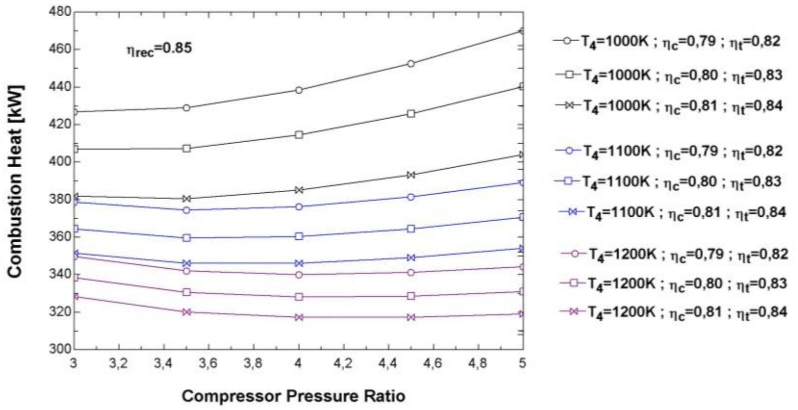

Figure 7. Combustion heat versus compressor pressure ratio.

It is observed that liquid power and combustion heat behave is similar to air mass flow for turbine inlet temperature and isentropic efficiencies, but reverse for compressor pressure ratio. It occurs because power turbine outlet temperature and recuperator outlet air temperature decreases as compressor pressure ratio increases (as shown in Fig. 2 and Fig. 3, respectively) and it causes an increase in enthalpy variation. Since power is defined by multiplication between flow mass and enthalpy variation and air mass flow decreases but power increases, it is concluded that this enthalpy variation effect is more significant for this case.

Since combustion heat increases as compressor pressure ratio too, the same is expected for electrical efficiency as shown in Fig. 8:

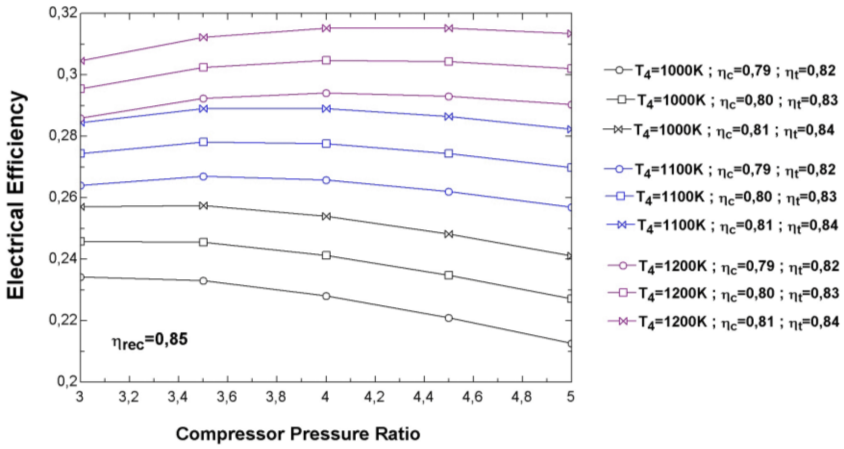

Figure 8. Electrical efficiency versus compressor pressure ratio.

Results for thermal efficiency are shown in Fig. 9:

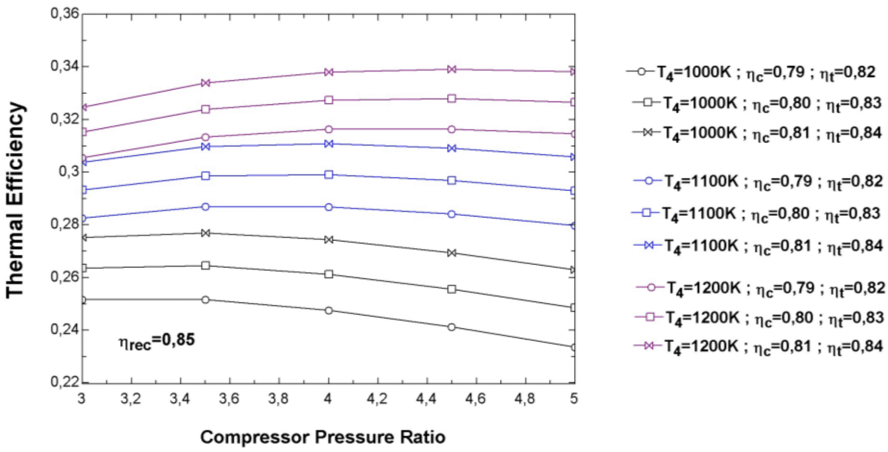

Figure 9. Thermal efficiency versus compressor pressure ratio.

For thermal efficiency, the trend is to occur less variation because liquid power and combustion heat increase as compressor pressure ratio increases too. However, there are moments when increase in one parameter is more significant than the other and it varies. Both efficiencies are higher for higher turbine inlet temperature and isentropic efficiencies since it causes higher enthalpy variation for liquid work and less enthalpy variation for combustion heat. The same occurs for recuperator efficiency.

Lastly, the effect of ambient temperature on electrical efficiency was investigated and is shown in Fig. 10:

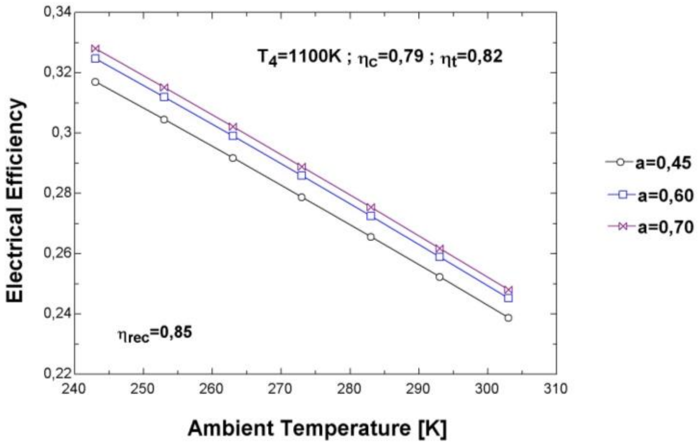

Figure 10. Electrical efficiency versus ambient temperature.

The decrease in electrical efficiency occurs as ambient temperature rises due to the decrease in air density that leads to higher compressor work and a decrease in power output could be expected. To maintain it constant, fuel mass flow is increased, leading to a larger heat input to the engine at a constant power output. This results, therefore, in lower efficiency (Somehsaraei et al., 2014). Futhermore, this graphic also shows higher electrical efficiency for higher methane percentage in biogas. This occurs because less fuel is necessary to achieve the same power output.

5. CONCLUSIONS

In this work a research was done to describe how MGT works, its thermodynamic equations, the advantages of using biogas and how parameters relate to each other through EES Demo graphics and parametric tables in order to search the best combination of them that leads to highest efficiencies and lowest fuel consumption for a 100 kWe biogas-fueled micro gas turbine. Good efficiencies were found and validated with the other works referenced. The best operation point occurs for highest values of turbine inlet temperature, recuperator efficiency, turbine and compressor isentropic efficiencies, percentage of methane and when compressor pressure ratio is about 4. For these values, electrical efficiency, thermal efficiency and specific fuel consumption are equal to approximately 31.9%, 34.1% and 0.47 kg/kWh.

6. ACKNOWLEDGEMENTS

The authors would like to thank Brazilian people, Federal University of Ouro Preto, FAPEMIG and Gorceix Foundation.

7. REFERENCES

Adefarati, T. and Bansal, R.C., 2016. “Integration of renewable distributed generators into the distribution system: a review”. *Renewable Power Generation*, Vol. 10, No. 7, pp. 873-884.

Adefarati, T. and Bansal, R.C., 2017. “Reliability and economic assessement of a microgrid power system with the integration of renewable energy resources”. *Applied Energy*, Vol. 206, pp. 911-933.

Borglin, S.H., 1991. “A contribuition to the calculation of open gas turbine processes”. *ASME COGEN-TURBO*, Vol. 6, pp. 115-129.

Çengel, Y.A. and Boles, M.A., 2006. “Thermodynamics: An Enginering Approach”. Book, 5th ed.

Gupta, K.K., Sidiqui, A.R. and Sarviya, R.M., 2010. “Bio-fuels for the gas turbine: A review”. *Renewable and Sustainable Energy Reviews*, Vol. 14, No. 9, pp. 2946-2955.

Ismail, M.S., Moghavvemi, M. and Mahlia, T.M.I., 2013. “Current utilization of microgasturbine as a part of a hybrid system in distributed generation technology”. *Renewable Power Generation*, Vol. 21, pp. 142-152.

Malinowski, L., Lewandowska, M., 2013. “Analytical model-based energy and exergy analysis of a gas microturbine at part-load operation”. *Applied Thermal Engineering*, Vol. 57, pp. 125-132.

MosayebNezhad, M., Mehr, A.S., Lanzini, A., Misual, D. and Santarelli, M., 2019. "Technology review and thermodynamic perfomance study of a biogas-fed micro humid air turbine". *Renewable Energy*, Vol. 140, pp. 407-418.

Shukla, T., 2013. "Micro Gas Turbine – A Review". *International Journal on Theoretical and Applied Research in Mechanical Engineering*, Vol. 2, Issue 3.

Somehsaraei, H.N., Majoumerd, M.M., Breuhaus, P. and Assadi, M., 2014. "Performane analysis of a biogas-fueled micro gas turbine using a validated thermodynamic model". *Applied Thermal Engineering*, Vol. 66, pp. 181-190.

Xiao, G., Yang, T., Liu, H., Ni, D., Ferrari, M.L., Li, M., Luo, Z., Cen, K. and Ni, M., 2017. "Recuperators for micro gas turbines: A review". *Applied Energy*, Vol. 197, pp. 83-99.

8. RESPONSIBILITY NOTICE

The authors are the only responsible for the printed material included in this paper.